

CO Cameron band and CO₂⁺ UV doublet emissions in the dayglow of Venus: Role of CO in the Cameron band production

Anil Bhardwaj¹ and Sonal Kumar Jain¹

Received 25 September 2012; revised 16 May 2013; accepted 17 May 2013; published 17 June 2013.

[1] The present study deals with the model calculations of CO Cameron band and CO₂⁺ ultraviolet doublet emissions in the dayglow of Venus. The overhead and limb intensities of CO Cameron band and CO₂⁺ UV doublet emissions are calculated for low, moderate, and high solar activity conditions. Using updated cross sections, the impact of different e-CO cross sections for Cameron band production is estimated. The electron impact on CO is the major source mechanism of Cameron band, followed by electron and photon impact dissociation of CO₂. The overhead intensities of CO Cameron band and CO₂⁺ UV doublet emissions are about a factor of 2 higher in solar maximum than those in solar minimum condition. The effect of solar EUV flux models on the emission intensity is ~30–40% in solar minimum condition and ~2–10% in solar maximum condition. At the altitude of emission peak (~135 km), the model predicted limb intensity of CO Cameron band and CO₂⁺ UV doublet emissions in moderate ($F_{10.7} = 130$) solar activity condition is about 2400 and 300 kR, respectively, which is in agreement with the very recently published SPICAV/Venus Express observation. The model limb intensity profiles of CO Cameron band and CO₂⁺ UV doublet are compared with SPICAV observation. We also calculated intensities of N₂ Vegard-Kaplan UV bands and O I 2972 Å emissions during moderate and high solar activity conditions.

Citation: Bhardwaj, A., and S. K. Jain (2013), CO Cameron band and CO₂⁺ UV doublet emissions in the dayglow of Venus: Role of CO in the Cameron band production, *J. Geophys. Res. Space Physics*, 118, 3660–3671, doi:10.1002/jgra.50345.

1. Introduction

[2] Several spacecraft, viz., Mariner 5 (three-channel photometer: 1050–2200 Å, 1250–2200 Å, and 1350–2200 Å), Venera 4 (1050–1340 Å and 1225–1340 Å), Mariner 10 (200–1700 Å), Venera 9 and 10 (visible spectrometers 3000–8000 Å and Lyman α filter photometer), Venera 11 and 12 (300–1700 Å), Pioneer Venus Orbiter (1100–1800 Å and 1600–3300 Å), and Cassini (561–1182 Å and 1155–1913 Å), have visited Venus so far. A review of past observations of Venus missions is given by Fox and Bougher [1991]. Currently, the Venus Express (VEx) is orbiting Venus, which has an experiment (SPICAV, 1100–3100 Å, 7000–17,000 Å, and 23,000–42,000 Å) for aeronomical studies of Venusian atmosphere. The major emission detected in the dayglow of Venus includes He I 584 Å and He II 304 Å lines, O I 989 Å, O I 1304 Å triplet, O I 1356 Å, O I 2972 Å, O II 834 Å, C I 1561 and 1657 Å, H Lyman- α , and CO fourth positive and Hopfield-Birge bands [e.g., Broadfoot et al., 1974,

1977; Bertaux et al., 1981; LeCompte et al., 1989; Gérard et al., 2011a, 2011b; Hubert et al., 2012].

[3] Theoretical calculations have shown CO Cameron band to be one of the brightest features (18–20 kR overhead intensity for low solar activity condition) in the UV dayglow of Venus [Fox and Dalgarno, 1981; Fox and Bougher, 1991; Gronoff et al., 2008]. The production sources of CO Cameron band ($a^3\Pi - X^1\Sigma^+$) on Venus are expected to be similar to those on Mars, viz., photon and electron impact dissociation of CO₂, dissociative recombination (DR) of CO₂⁺, and electron impact on CO (e-CO). Since $X^1\Sigma^+ \rightarrow a^3\Pi$ is a forbidden transition, resonance fluorescence of CO is not an effective excitation mechanism. The CO₂⁺ UV doublet emission originates due to transition from $B^2\Sigma_u^+$ state of CO₂⁺ to the ground state ($B^2\Sigma^+ - X^2\Pi$). Theoretical calculations predicted an overhead dayglow intensity of around 7–10 kR for UV doublet, with photoionization being the dominant production mechanism [Fox and Dalgarno, 1981; Gronoff et al., 2008].

[4] The main objective of the present study is to understand the role of various processes governing the production of CO Cameron band and CO₂⁺ UV doublet emissions in the dayglow of Venus in the light of updated cross sections and reaction rates. Recently, we have developed a model for the CO Cameron band and CO₂⁺ UV doublet emissions in the dayglow of Mars [Jain and Bhardwaj, 2012]. In the present study, this model is applied to Venus to calculate the CO

¹Space Physics Laboratory, Vikram Sarabhai Space Centre, Trivandrum, India.

Corresponding author: S. K. Jain, Space Physics Laboratory, Vikram Sarabhai Space Centre, Trivandrum 695022, India. (sonaljain.spl@gmail.com)

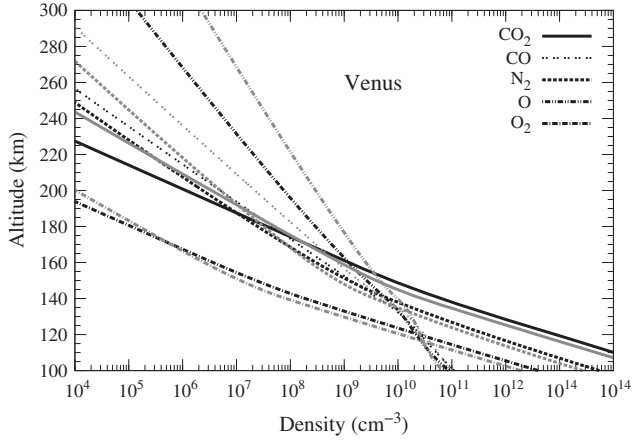


Figure 1. Model atmosphere of Venus for low (black curves) and high solar (grey curves) activity conditions.

Cameron band and CO_2^+ UV doublet dayglow emissions for low, moderate, and high solar activity conditions.

[5] After submission of this paper, the first observation of CO Cameron band and CO_2^+ UV doublet emissions in the dayglow of Venus using the SPICAV aboard Venus Express was reported [Chaufray *et al.*, 2012]. Keeping the structure of the paper unchanged, we added a section in the revised version, where we compared model prediction with the SPICAV observation. Details of the model are given in section 2, followed by results and discussion in sections 3 and 4, respectively. The summary and conclusions are presented in section 6.

2. Development of Model

[6] Primary photoelectron production rate is calculated using

$$Q(Z, E) = \sum_l n_l(Z) \sum_{j,\lambda} \sigma_l^I(j, \lambda) I(Z, \lambda) \delta\left(\frac{hc}{\lambda} - E - W_{jl}\right) \quad (1)$$

$$I(Z, \lambda) = I(\infty, \lambda) \exp\left[-\sec(\chi) \sum_l \sigma_l^A(\lambda) \int_Z^\infty n_l(Z') dZ'\right] \quad (2)$$

where σ_l^A and $\sigma_l^I(j, \lambda)$ are the total photoabsorption cross section and the photoionization cross section of the j th ion state of the constituent l at wavelength λ , respectively; $I(\infty, \lambda)$ is the unattenuated solar flux at wavelength λ ; n_l is the neutral density of constituent l at altitude Z ; χ is the solar zenith angle (SZA); $\delta(hc/\lambda - E - W_{jl})$ is the delta function, in which hc/λ is the incident photon energy; W_{jl} is the ionization potential of the j th ion state of the l th constituent; and E is the energy of ejected electron.

[7] To calculate the photoelectron flux, we have adopted the Analytical Yield Spectra (AYS) technique [cf. Bhardwaj *et al.*, 1990; Singhal and Bhardwaj, 1991; Bhardwaj, 1999, 2003]. The AYS technique is an analytical representation of numerical yield spectra obtained using the Monte Carlo model [cf. Singhal *et al.*, 1980; Singhal and Bhardwaj, 1991; Bhardwaj and Michael, 1999; Bhardwaj and Jain, 2009].

Using AYS, the photoelectron flux has been calculated as

$$\phi(Z, E) = \int_{W_{kl}}^{100\text{eV}} \frac{Q(Z, E) U(E, E_0)}{\sum_l n_l(Z) \sigma_{IT}(E)} dE_0 \quad (3)$$

where $\sigma_{IT}(E)$ is the total inelastic cross section for the l th gas with density n_l and $U(E, E_0)$ is the two-dimensional AYS, which embody the nonspatial information of degradation process. It represents the equilibrium number of electrons per unit energy at an energy E resulting from the local energy degradation of an incident electron of energy E_0 . For the CO_2 gas, the AYS are taken from Bhardwaj and Jain [2009], and for other gases, viz., O_2 , N_2 , O , and CO , we have used the AYS given by Singhal *et al.* [1980]. The ion and electron temperatures for solar minimum and maximum conditions are taken from Fox [2009].

[8] Model atmosphere (considering CO_2 , N_2 , CO , and O) of Venus is taken from the VTS3 model of Hedin *et al.* [1983] for solar minimum ($F_{10.7} = 60$), moderate ($F_{10.7} = 130$), and maximum ($F_{10.7} = 200$) conditions, for equatorial region and local time of 1500 h, which corresponds to the solar zenith angle of around 45° . Based on the study of Fox and Bougher [1991], the density of O_2 is taken as 3×10^{-3} times that of CO_2 density. Figure 1 shows the model atmosphere of Venus for low and high solar activity conditions. Below 160 km (150 km in case of high solar activity), CO_2 is the major atmospheric species, but above this altitude, atomic oxygen becomes the dominant neutral in the atmosphere of Venus.

[9] In the present study, solar EUV flux from EUVAC model [Richards *et al.*, 1994] is used for low, moderate, and high solar activity conditions. To assess the impact of solar EUV flux model on the calculated intensities, the solar EUV flux from SOLAR2000 (S2K) v2.36 model [Tobiska, 2004] is also used. The solar EUV flux is taken at 1 AU and then scaled to the Sun-Venus distance (0.72 AU). There are

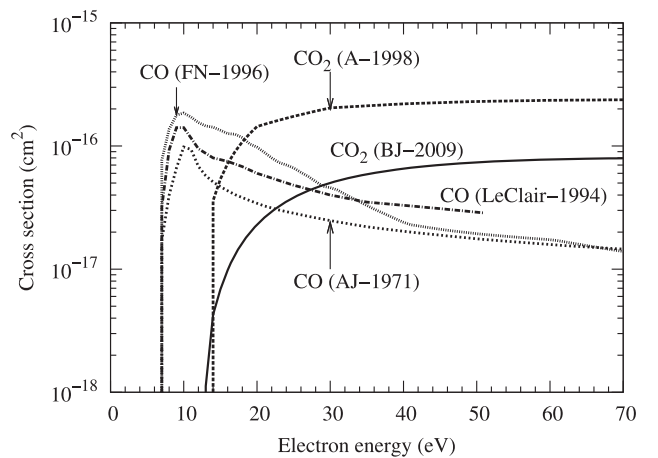


Figure 2. Cross sections for the production of $\text{CO}(a^3\Pi)$ due to electron impact on CO and CO_2 . A-1998, BJ-2009, FN-1996, LeClair-1994, and AJ-1971 refer to Avakyan *et al.* [1998], Bhardwaj and Jain [2009], Furlong and Newell [1996], LeClair *et al.* [1994], and Ajello [1971b], respectively. BJ-2009 cross section is plotted after dividing it by a factor of 3.

Table 1. CO($a^3\Pi$) and CO $_2^+(B^2\Sigma_u^+)$ Production Processes and References for Cross Sections and Reaction Rates^a

Process	References
CO $_2 + e_{ph} \rightarrow$ CO($a^3\Pi$) + O	<i>Bhardwaj and Jain</i> [2009]
CO $_2 + h\nu \rightarrow$ CO($a^3\Pi$) + O	<i>Lawrence</i> [1972]
CO $_2^+ + e_{th} \rightarrow$ CO($a^3\Pi$) + O	<i>Seiersen et al.</i> [2003]; <i>Skrzypkowski et al.</i> [1998]
CO + $e_{ph} \rightarrow$ CO($a^3\Pi$)	<i>Furlong and Newell</i> [1996] ^a
CO $_2 + e_{ph} \rightarrow$ CO $_2^+(B^2\Sigma_u^+)$	<i>Bhardwaj and Jain</i> [2009]
CO $_2 + h\nu \rightarrow$ CO $_2^+(B^2\Sigma_u^+)$	<i>Schunk and Nagy</i> [2000] ^b
CO $_2^+ + h\nu \rightarrow$ CO $_2^+(B^2\Sigma_u^+)$	<i>Dalgarno and Degges</i> [1971]

^aCross section measured by *LeClair et al.* [1994] has also been used.

^bBranching ratios for ionization in different states are from *Avakyan et al.* 1998.

substantial differences in the solar EUV fluxes of EUVAC and S2K models; moreover, these differences are not similar in solar minimum and maximum conditions [e.g., see *Jain and Bhardwaj*, 2012; *Bhardwaj and Jain*, 2012a]. In both solar minimum and maximum conditions, the solar flux estimated in bins is higher in S2K than in EUVAC over the entire range of wavelengths, except for the bins below 250 Å (150 Å for solar minimum condition), whereas solar fluxes at prominent lines are higher in EUVAC model for entire wavelength range [see *Jain and Bhardwaj*, 2012, Figure 1]. The higher solar fluxes above 250 Å in S2K cause more photoionization. Higher photon fluxes below 250 Å (during solar maximum condition) in EUVAC model produce more high energy electrons causing secondary ionizations that can compensate for the higher photoionization in S2K model. A major difference between solar EUV flux of S2K and EUVAC models is the solar flux at bin (1000–1050 Å) containing H Ly- β (1026 Å) line, which in both solar conditions is around an order of magnitude higher in S2K compared to EUVAC solar flux model. The solar fluxes at longer wavelength are very important for dissociative excitation processes. Hence, contribution of photodissociation (PD) of CO $_2$ in CO($a^3\Pi$) production would be higher when the S2K solar EUV flux model is used.

[10] Due to its long lifetime, cross section for the production of CO($a^3\Pi$) due to electron impact dissociation of CO $_2$ (e-CO $_2$) is difficult to measure in the laboratory. *Ajello* [1971a] reported relative magnitudes of the cross section for the (0, 1) transition of CO Cameron band at 215.8 nm and reported a value of 1×10^{-17} cm 2 at 80 eV. *Erdman and Zipf* [1983] later criticized the cross section obtained by *Ajello* [1971a] and advocated a value of 9×10^{-17} cm 2 at 80 eV due to a re-evaluation to 9 ms of the radiative lifetime [*Johnson*, 1972]. They subsequently multiplied this value by a factor of 2.7 to account for higher mean velocity of CO($a^3\Pi$) fragments, which might have escaped detection [*Wells et al.*, 1972]. Therefore, *Erdman and Zipf* [1983] reported a value of 2.4×10^{-16} cm 2 at 80 eV. *Avakyan et al.* [1998] have estimated the CO Cameron band cross section based on the cross section of *Ajello* [1971a] with the correction of *Erdman and Zipf* [1983]. *Bhardwaj and Jain* [2009] have analytically fitted the cross section of CO($a^3\Pi$) production due to electron impact on CO $_2$ using the suggested value of *Erdman and Zipf* [1983].

[11] *Conway* [1981] constructed a synthetic spectrum of Martian dayglow between 1800 and 2600 Å. Based on the comparison of the model calculation with Mariner observa-

tion, *Conway* found that a cross section with a maximum value of 7×10^{-17} cm 2 was consistent with the data. The value suggested by *Conway* [1981] is around a factor of 3 smaller than that of *Erdman and Zipf* [1983]. Recent comparison between calculations and observations of dayglow emission on Mars suggests a lower value of e-CO $_2$ cross sections for the CO Cameron band production [*Simon et al.*, 2009; *Jain and Bhardwaj*, 2012; *Gronoff et al.*, 2012]. *Jain and Bhardwaj* [2012] and *Gronoff et al.* [2012] have shown that Cameron band cross sections of *Erdman and Zipf* [1983] should be reduced by a factor of 2 to 3, to bring the calculated CO Cameron band intensities in agreement with the Mars Express observation. The reduction in the CO($a^3\Pi$) cross section is also supported by recent measurements of radiative lifetime of CO($a^3\Pi$). Based on theoretical and experimental work, *Gilijamse et al.* [2007] have re-analyzed the radiative lifetime of CO($a^3\Pi$), and reported a value of ~ 3.16 ms, which is around 3 times less than the value of *Johnson* [1972]. In the present study, the cross section for CO($a^3\Pi$) production due to electron impact on CO $_2$ is taken from *Bhardwaj and Jain* [2009] after dividing it by a factor of 3, which is shown in Figure 2 along with the recommended cross section of *Avakyan et al.* [1998].

[12] Electron impact on CO (e-CO) is also a source of CO Cameron band. On Mars, due to less abundance of CO, it does not contribute significantly to the total Cameron band emission [*Fox and Dalgarno*, 1979; *Jain and Bhardwaj*, 2012]. However, on Venus, CO contribution cannot be neglected due to its relatively larger abundance above 150 km (cf. Figure 1). In comets, where the CO abundance is larger or equal to that of the CO $_2$, the major contribution to CO Cameron band emission is from electron impact on CO [*Bhardwaj and Raghuram*, 2011; *Raghuram and Bhardwaj*, 2012]. In the previous calculations of CO Cameron band emission in the dayglow of Venus [*Gronoff et al.*, 2008; *Fox and Dalgarno*, 1981; *Fox and Bougher*, 1991], the

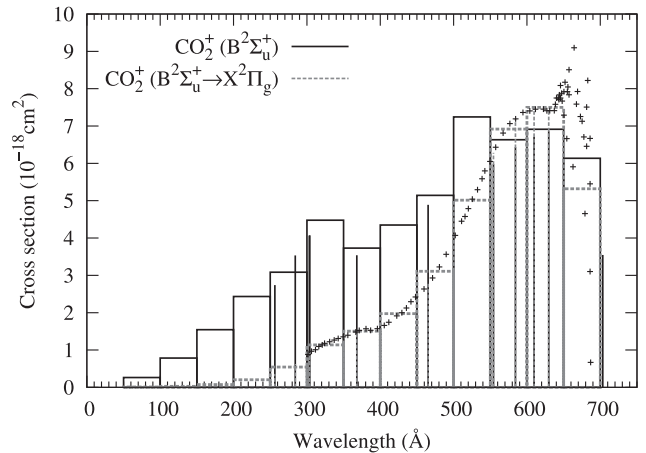


Figure 3. Photon impact excitation cross section of CO $_2^+(B^2\Sigma_u^+)$ taken from *Schunk and Nagy* [2000] with branching ratio from *Avakyan et al.* [1998] (black lines). Symbols show the emission cross section of CO $_2^+(B^2\Sigma_u^+ \rightarrow X^2\Pi_g)$ as given in *Ukai et al.* [1992]. Grey lines show the emission cross section of CO $_2^+(B^2\Sigma_u^+ \rightarrow X^2\Pi_g)$ averaged at 37 wavelengths bins; at wavelengths below 300 Å, cross section is extrapolated.

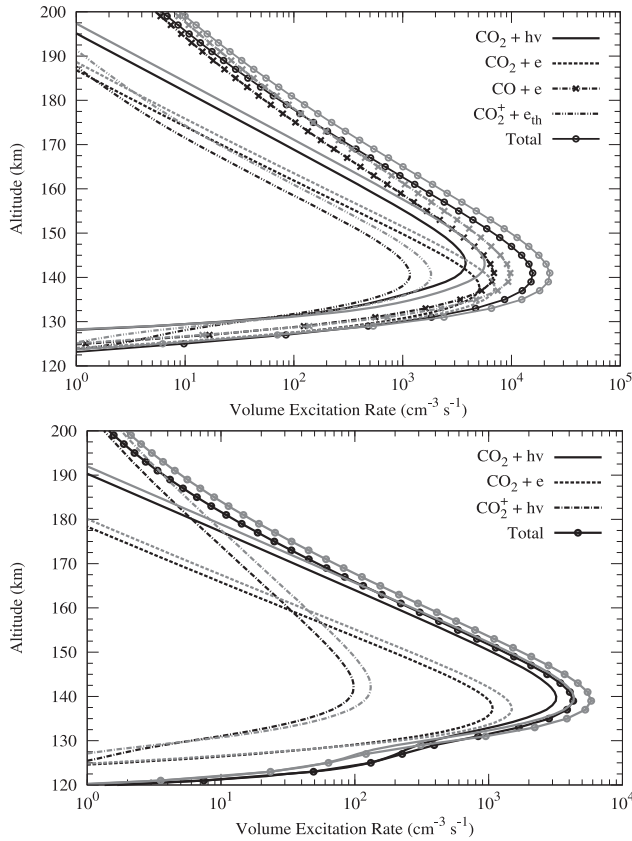


Figure 4. Calculated production rates of the (top) $\text{CO}(a^3\Pi)$ and (bottom) $\text{CO}_2^+(B^2\Sigma_u^+)$ on Venus for low solar activity condition at $\text{SZA} = 45^\circ$. Black curves show production rates calculated using EUVAC model while grey curves show them for S2K solar flux model.

e-CO cross section for $\text{CO}(a^3\Pi)$ production was taken from the work of *Ajello* [1971b]. *Ajello* [1971b] used the (1,4) Cameron band at 2389 \AA to normalize the entire band system cross section in electron impact excitation of CO. However, according to *Erdman and Zipf* [1983], the (1,4) Cameron band was contaminated by (6,16) CO fourth positive band. *Erdman and Zipf* [1983] repeated and re-analyzed *Ajello's*

experiment with higher sensitivity and concluded that total cross-section value ($1.1 \times 10^{-16} \text{ cm}^2$ at 11 eV) measured by *Ajello* [1971b] should, therefore, be reduced by a factor of 8 to an apparent value of $1.4 \times 10^{-17} \text{ cm}^2$ at 11 eV. In addition to the contamination problem, *Ajello's* total Cameron band emission cross section was based on the assumption of radiation lifetime of 1 ms for $a^3\Pi$ state. *Erdman and Zipf* [1983] used the radiative life of 9 ms [*Johnson, 1972*] and multiplied the cross section (already corrected for contamination) by a factor of 9 and gave a cross-section value of $1.5 \times 10^{-16} \text{ cm}^2$ at 11 eV, with an uncertainty close to 75%.

[13] After accounting for corrections, the cross-section value suggested by *Erdman and Zipf* [1983] is very close to the cross section of *Ajello* [1971b]. However, based on $\text{CO}(a^3\Pi)$ radiative lifetime of ~ 3 ms reported by *Gilijamse et al.* [2007], the Cameron band cross section in e-CO process should be reduced by a factor of 3.

[14] *LeClair et al.* [1994] have measured the e-CO cross section for $\text{CO}(a^3\Pi)$ production using solid xenon detector and time of flight technique. *LeClair et al.* [1994] have given the integral cross section of $\text{CO}(a^3\Pi)$ —that includes cascading contributions from higher triplet states—by normalizing their excitation function to the maximum absolute cross section ($1.5 \times 10^{-16} \text{ cm}^2$ at 11 eV) obtained by *Erdman and Zipf* [1983]. This normalization may cause an overestimation of $\text{CO}(a^3\Pi)$ section measured by *LeClair et al.* [1994], since *Erdman and Zipf* [1983] have used the radiative lifetime of 9 ms, which is a factor of 3 higher than recently measured lifetime of 3 ms [*Gilijamse et al., 2007*]. The shape of normalized $\text{CO}(a^3\Pi)$ cross section measured by *LeClair et al.* [1994] is identical to the one recorded by *Ajello* [1971b]. However, maximum cross section is at 9.4 eV in *LeClair et al.* [1994] measurement compared to 11 eV in *Ajello* [1971b] experiment. *LeClair et al.* [1994] attributed this difference in peak position to the electron beam characteristic in the two experiments.

[15] *Furlong and Newell* [1996] reported the absolute integral cross section for $\text{CO}(a^3\Pi)$ production in the e-CO collision by normalizing their measurements to maximum cross-section value ($1.698 \times 10^{-16} \text{ cm}^2$ at 8.5 eV) calculated by *Morgan and Tennyson* [1993]. Below 10 eV, their cross section is in good agreement with that of *LeClair et al.* [1994]. Above 10 eV, *Furlong and Newell* [1996] reported

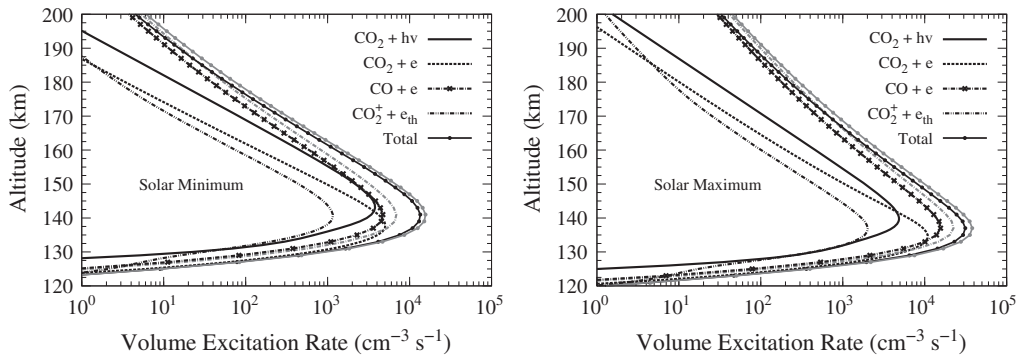


Figure 5. Calculated production rates of the $\text{CO}(a^3\Pi)$ on Venus for (left) low and (right) high solar activity conditions at $\text{SZA} = 45^\circ$. Black curves show production rates calculated using EUVAC model and the $\text{CO}(a^3\Pi)$ cross section in e-CO process from *LeClair et al.* [1994], while grey curves show the production rate of $\text{CO}(a^3\Pi)$ in e-CO process and total production rate when $\text{CO}(a^3\Pi)$ cross section is taken from *Furlong and Newell* [1996].

Table 2. Overhead Intensities (in kR) of CO Cameron Band and CO₂⁺ UV Doublet Emissions on Venus for Low, Moderate, and High Solar Activity Conditions at SZA = 45°^a

Process	Intensity (kR)					
	CO Cameron Band			CO ₂ ⁺ UV Doublet		
	Low SA ^b	Moderate SA ^c	High SA ^d	Low SA	Moderate SA	High SA
<i>EUVAC Solar Flux Model</i>						
CO ₂ + hν	5.7 (6.2) ^e	7.2	7.5	4.8	8.5	9.5
e _{ph} ⁻ + CO ₂	6.6 (7.8)	12.3	13.7	1.4	2.7	3
e _{ph} ⁻ + CO	11.4 [7.8] ^f (2.9)	27.3	36.3 [25.6]	-	-	-
e _{th} ⁻ + CO ₂ ⁺	1.7 (2)	2.9	2.9	-	-	-
FS	-	-	-	0.2	0.3	0.3
Total	25.3 [21.8] (18)	49.8	60.4 [49.8]	6.4 {4} ^g	11.5 {7.2}	12.8 {8}
<i>SOLAR2000 Solar Flux Model</i>						
CO ₂ + hν	8.6	10.7	11.6	6.3	8	8.7
e _{ph} ⁻ + CO ₂	9.2	11	11.7	1.9	2.4	2.5
e _{ph} ⁻ + CO	16.2	26.3	33.5	-	-	-
e _{th} ⁻ + CO ₂ ⁺	2.6	2.8	2.6	-	-	-
FS	-	-	-	0.4	0.3	0.3
Total	36.3	51	59.4	8.6 {5.5}	10.7 {6.7}	11.4 {7.2}

^ae_{ph}⁻ = photoelectron; e_{th}⁻ = thermal electron; FS = fluorescent scattering of CO₂⁺.

^bLow solar activity ($F_{10.7} = 60$).

^cModerate solar activity ($F_{10.7} = 130$).

^dHigh solar activity ($F_{10.7} = 200$).

^eCalculated values in parenthesis are for model atmosphere of *Fox and Dalgarno* [1981] and e-CO Cameron band production cross section from *Ajello* [1971b].

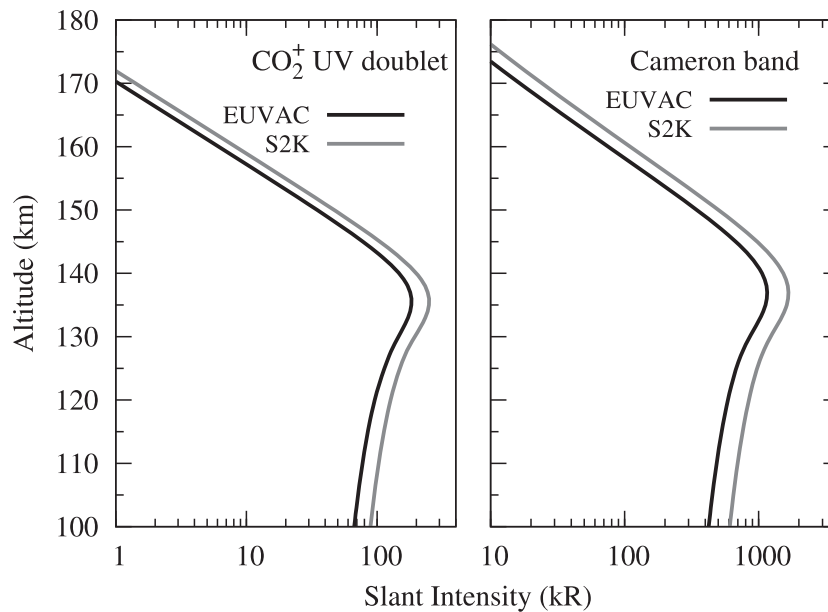
^fCalculated values in brackets are for the CO(*a*³Π) cross section of *LeClair et al.* [1994].

^gCalculated by taking the 50% crossover from B to A before radiating.

an increase in cross section due to the contribution from cascading into *a*³Π state. The cross sections obtained by *Furlong and Newell* [1996] are about a factor of 2 higher between 10 and 35 eV compared to that of *LeClair et al.* [1994].

[16] The above mentioned discussion clearly points out the difference in the cross section of CO(*a*³Π) in electron impact excitation of CO. In the present study, the cross section of *Furlong and Newell* [1996] is used for CO(*a*³Π)

production in e-CO collision. The cross section of *LeClair et al.* [1994] is also used to assess the effect of cross section in Cameron band intensity. The reason for using these two cross sections over the one measured by *Ajello* [1971b] is due to the fact that *Ajello*'s measured cross section has been shown to be flawed by *Erdman and Zipf* [1983]. Figure 2 depicts the CO(*a*³Π) cross sections in e-CO process used in the present study along with cross section obtained by *Ajello* [1971b]. The cross section of CO(*a*³Π) production in e-CO


Figure 6. Calculated limb profiles of (left) CO₂⁺ UV doublet and (right) CO Cameron band emissions for EUVAC and S2K solar EUV flux models for low solar activity condition at SZA = 45°.

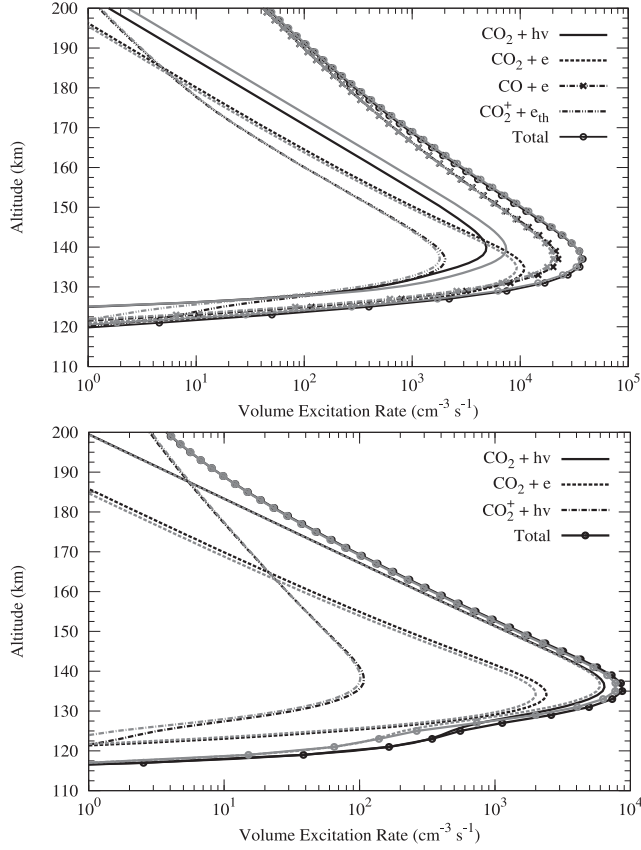


Figure 7. Calculated production rates of the (top) $\text{CO}(\text{a}^3\Pi)$ and (bottom) $\text{CO}_2^+(\text{B}^2\Sigma_u^+)$ for high solar activity condition at $\text{SZA} = 45^\circ$. Black curves show calculated production rates using EUVAC model while grey curves show them for S2K solar flux model.

process attains maximum value at ~ 10 eV, where photoelectron flux also has high values [Bhardwaj and Jain, 2012a]. This makes e-CO collisions more important for the Cameron band production, if CO density is sufficient, as in the case of Venus. At electron energies > 25 eV, $\text{CO}(\text{a}^3\Pi)$ cross section in e- CO_2 process becomes dominant (cf. Figure 2).

[17] The details of photoabsorption, photoionization, and electron impact cross sections used in the present study are given in our previous work [Jain and Bhardwaj, 2011, 2012, Bhardwaj and Jain, 2012a]. The details of cross sections and processes considered in the model to calculate CO Cameron band and CO_2^+ UV doublet emissions are summarized in Table 1. While calculating the emission from $\text{B}^2\Sigma_u^+$ state of CO_2^+ , we have taken branching ratio of 0.5 (for photoionization only) from the $\text{CO}_2^+(\text{B})$ to (A) based on the study of Fox and Dalgarno [1979]. Ukai et al. [1992] have given the direct emission cross section of $\text{CO}_2^+(\text{B}^2\Sigma_u^+ \rightarrow \text{X}^2\Pi_g)$ transition. This cross section is also used in the present study to assess the impact of using excitation and emission cross section of $\text{B}^2\Sigma_u^+$ state of CO_2^+ . Figure 3 shows the $\text{CO}_2^+(\text{B}^2\Sigma_u^+)$ excitation and $\text{CO}_2^+(\text{B}^2\Sigma_u^+ \rightarrow \text{X}^2\Pi_g)$ emissions cross sections due to photon impact on CO_2 . Emission cross section of Ukai et al. [1992] has been averaged at 37 wavelength bins. The contribution of fluorescence scattering of CO_2^+ to the UV doublet emission is calculated by taking the fluorescence efficiency (g) value of $5.2 \times 10^{-3} \text{ s}^{-1}$ for Venus [Dalgarno and Degges, 1971].

3. Results

3.1. Solar Minimum Condition

[18] Figure 4 shows the calculated volume excitation rates of $\text{CO}(\text{a}^3\Pi)$ and $\text{CO}_2^+(\text{B}^2\Sigma_u^+)$ for low solar activity condition. The altitude of peak production is ~ 140 km. The major production source of Cameron band at the peak is e-CO process, whose contribution is about 44%; unlike on Mars, where electron impact on CO_2 is the major Cameron

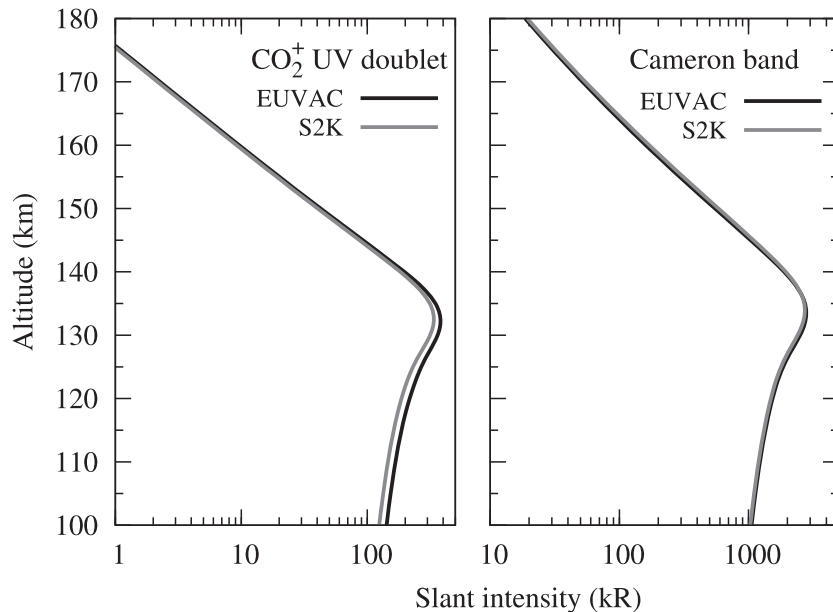


Figure 8. Calculated limb profiles of (left) CO_2^+ UV doublet and (right) CO Cameron band for EUVAC and S2K solar EUV flux models for high solar activity condition at $\text{SZA} = 45^\circ$.

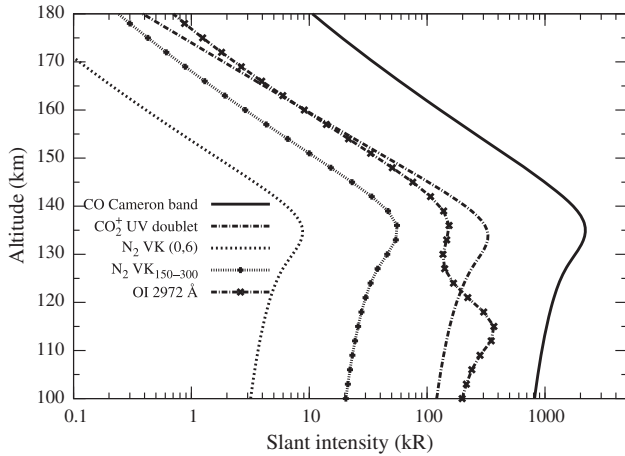


Figure 9. The calculated (using EUVAC solar flux model) limb profiles of CO_2^+ UV doublet and CO Cameron band emissions for moderate solar activity condition at $\text{SZA} = 45^\circ$. The calculated limb intensities of O I 2972 Å and N_2 VK (0, 6) emission are also shown in the figure, along with the limb intensity of N_2 VK band in wavelength region 1500–3000 Å.

band production mechanism [Jain and Bhardwaj, 2012]. Table 2 shows the height-integrated overhead intensity of CO Cameron band with contributions of different sources. The e-CO collisions are the major source of Cameron band production with contribution of around 45%, followed by e- CO_2 , PD of CO_2 , and DR of CO_2^+ , whose contributions are around 25%, 23%, and 7%, respectively.

[19] Figure 4 (bottom) shows the volume production rate of $\text{CO}_2^+(\text{B}^2\Sigma_u^+)$, and the height-integrated overhead intensity of CO_2^+ UV doublet emission for different sources is presented in Table 2. Photoionization of CO_2 is the dominant source (75%) of $\text{CO}_2^+(\text{B}^2\Sigma_u^+)$ production, followed by the electron impact ionization of CO_2 (21%). Contribution of fluorescent scattering of CO_2^+ is very small ($\sim 3\%$).

[20] Figure 5 shows the volume production rate of $\text{CO}(\text{a}^3\Pi)$ for low and high solar activity conditions calculated by using the $\text{CO}(\text{a}^3\Pi)$ cross section measured by LeClair *et al.* [1994]. The height-integrated intensity of Cameron band is given in Table 2. The e-CO process is still the dominant source of Cameron band production, though its contribution in Cameron band production is reduced compared to the case when $\text{CO}(\text{a}^3\Pi)$ cross section is taken from Furlong and Newell [1996], which is consistent with our previous considerations.

[21] The volume excitation rates are integrated along the line of sight to calculate the limb intensities of CO_2^+ UV doublet and CO Cameron band emissions in the dayglow of Venus. Limb intensity at each tangent point is calculated as

$$I = 2 \int_0^\infty V(r) dr \quad (4)$$

where r is abscissa along the horizontal line of sight and $V(r)$ is the volume emission rate (in $\text{cm}^{-3} \text{s}^{-1}$) at a particular emission point r . The factor of 2 multiplication comes due to symmetry along the line of sight with respect to the tangent point. While calculating limb intensity, we assumed that the emission rate is constant along local longitude/latitude.

Figure 6 shows the limb intensities of CO_2^+ UV doublet and CO Cameron band emission on Venus. The calculated limb intensity of Cameron band peaks at 137 km with a value of 1200 kR, while the maximum limb intensity of CO_2^+ UV doublet emission is 183 kR at an altitude of 136 km.

3.2. Solar Maximum Condition

[22] Figure 7 shows the calculated volume excitation rates of (top) CO Cameron band and (bottom) CO_2^+ UV doublet emissions for solar maximum condition. The production rate of Cameron band attains a maximum value of $3.8 \times 10^4 \text{ cm}^{-3} \text{ s}^{-1}$ at an altitude of 137 km. The height-integrated overhead intensity is presented in Table 2. Electron impact on CO is by far the dominant production source of Cameron band contributing about 60%, followed by electron impact on CO_2 (23%), PD of CO_2 (12%), and DR of CO_2^+ (4%). The $\text{CO}(\text{a}^3\Pi)$ production rate calculated using e-CO cross section from LeClair *et al.* [1994] is shown in Figure 5 and corresponding height-integrating intensities in Table 2.

[23] For the CO_2^+ UV doublet emission, maximum production rate occurs at an altitude of 135 km with a value of $\sim 8.7 \times 10^3 \text{ cm}^{-3} \text{ s}^{-1}$ (cf. Figure 7). The overhead intensity of CO_2^+ UV doublet is presented in Table 2. The PD of CO_2 is the dominant (74%) production source of UV doublet emission followed by electron impact on CO_2 (23%) and fluorescent scattering by CO_2^+ (3%). Figure 8 shows the calculated line of sight intensities of CO Cameron band and CO_2^+ UV doublet emissions. The intensity of Cameron band peaks ~ 135 km with a value of 2700 kR, while the intensity of UV doublet emission attains a maximum value of around 380 kR at an altitude of 132 km.

3.3. Solar Moderate Condition

[24] The model calculation is also carried out for the moderate solar activity condition by taking the solar EUV flux on 1 July 2012 ($F_{10.7} = 130$). The height-integrated overhead intensities of CO Cameron band and CO_2^+ UV doublet emissions are presented in Table 2. Our calculation shows that for solar moderate condition also, the e-CO process is the dominant mechanism of CO Cameron band production contributing about 55%, followed by electron impact on CO_2 (25%), PD of CO_2 (14%), and DR of CO_2^+ (6%). The PD of CO_2 is the dominant (74%) production source of UV doublet emission followed by electron impact on CO_2 (23%) and fluorescent scattering by CO_2^+ (3%). Figure 9 shows the calculated limb intensities of CO Cameron band and CO_2^+ UV doublet emissions in the dayglow of Venus for moderate solar activity condition. Both emissions maximize at ~ 135 km with intensity of ~ 2200 kR for CO Cameron band and 330 kR for CO_2^+ UV doublet emission.

4. Discussion

[25] The present model calculation shows that the electron impact on CO is the dominant source of CO Cameron band production in the atmosphere of Venus for low, moderate, and high solar activity conditions using the $\text{CO}(\text{a}^3\Pi)$ cross sections of Bhardwaj and Jain [2009] and Furlong and Newell [1996] in electron impact on CO_2 and CO, respectively. For solar minimum condition Fox and Dalgarno [1981] and Gronoff *et al.* [2008] reported that e- CO_2 process is the major production source of Cameron band. Gronoff

et al. [2008] have calculated CO Cameron band intensity of 17.3 kR, with 7 kR from electron impact on CO₂, 5.3 kR from PD of CO₂, 4 kR from electron impact on CO, and 1 kR from DR of CO₂⁺. *Gronoff et al.* [2008] have used the cross section of *Ajello* [1971b] for electron impact on CO, while in the present study, the cross section of *Furlong and Newell* [1996] has been used. Using the cross section of *Ajello* [1971b], our model-calculated overhead Cameron band intensity is 18.6 kR, with contributions from e-CO₂, PD of CO₂, e-CO, and DR of CO₂⁺ processes being 6.7, 5.6, 4.6, and 1.7 kR, respectively. The model-calculated total CO Cameron band intensity is in good agreement with that of *Gronoff et al.* [2008]. *Fox and Dalgarno* [1981] reported the Cameron band intensity of about 20 kR, with contribution of ~25% from DR of CO₂⁺ and 6% from e-CO process. The present calculation, as well as that of *Gronoff et al.* [2008], shows that the contribution of DR of CO₂⁺ (which depends on electron density and temperature) is smallest among the processes considered in the model (see Table 2). *Fox and Bougher* [1991] suggested that the source of DR was overestimated in the pre-Pioneer Venus model of *Fox and Dalgarno* [1981] because of low density of atomic oxygen, which led to larger densities of CO₂⁺ ion. The mixing ratio of CO was lower in the model atmosphere used by *Fox and Dalgarno* [1981], whereas in the present calculation, as well as in the model of *Gronoff et al.* [2008], the VTS3 model atmosphere is used, which has larger CO mixing ratio. To evaluate the effect of low CO mixing ratio, the model calculation is also carried out by taking the model atmosphere of *Fox and Dalgarno* [1981]; the results are shown in Table 2. The Cameron band intensity is 18 kR when the model atmosphere of *Fox and Dalgarno* [1981] and e-CO cross section of *Ajello* [1971b] are used, which is in agreement with the model result of *Fox and Dalgarno* [1981]. However, in the present calculation, the contribution of DR is about 11%, which is lower than that reported by *Fox and Dalgarno* [1981]; this might be due to the difference in DR rate coefficient for CO(a³Π) production in the two calculations.

[26] For solar maximum condition, *Fox and Bougher* [1991] have reported total Cameron band intensity of 57 kR, which is in agreement with the value of 60 kR in the present study. However, the contribution of individual processes is different in the two studies. In the present study, the e-CO is the dominant process, whereas in the model calculation of *Fox and Bougher* [1991], the photon and electron impact on CO₂ played the dominant role with contribution of about 36% from each, while the contributions of electron impact on CO and DR of CO₂⁺ were 20% and 8%, respectively.

[27] The present study shows that the contribution of e-CO process in CO(a³Π) production is directly related to the cross section used in the calculation. For CO(a³Π) cross section of *LeClair et al.* [1994], the e-CO process is found to be the dominant source of CO Cameron band (see Figure 5 and Table 2). Overall, the calculation shows that the role of electron impact on CO in the Cameron band production may have been underestimated in the earlier calculations of *Fox and Dalgarno* [1981] and *Gronoff et al.* [2008] due to the choice of e-CO cross section for CO(a³Π) production used in their calculations.

[28] It has been mentioned earlier that a branching ratio of 0.5 has been used to calculate the UV doublet emission

intensity because we have used excitation cross section of CO₂⁺(B) in the calculation. However, if emission cross section of CO₂(B) given by *Ukai et al.* [1992] is used in the calculation rather than the excitation cross section, the contribution of photoionization in CO₂⁺(B²Σ_u⁺) ion production reduces by about 30%. For example, during solar minimum (maximum) condition, the overhead intensity of UV doublet emission due to photoionization of CO₂ is about 1.8 kR (2.8 kR). This value is about 25% (40%) smaller than that calculated using CO₂(B) excitation cross section (if 50% branching crossover from B to A state is considered for excitation cross section). It shows that use of emission and excitation cross sections of CO₂(B) affects the emission intensity of CO₂⁺ UV doublet.

4.1. Effect of Solar EUV Flux Models

[29] During the solar minimum condition, the CO Cameron band excitation rate calculated using the S2K model is about 45% larger than that calculated using the EUVAC model, while the production in PD of CO₂ is about 50% higher when S2K model is used. However, the altitude of peak production is same for both solar EUV flux models (see Figure 4). The limb intensities calculated using the S2K model are about 40% larger than those calculated using the EUVAC model (see Figure 6).

[30] For high solar activity condition, the intensity of CO Cameron band and CO₂⁺ UV doublet emissions calculated using the EUVAC model is about 2% and 10%, respectively, higher than those calculated using the S2K model. This is due to the higher solar EUV flux in EUVAC model at wavelengths ≤250 Å that produces energetic photoelectrons which further ionize the medium and compensate for the higher photoionization by solar EUV flux at wavelengths >250 Å in the S2K model. The effect of solar EUV flux on model calculations for moderate solar activity condition is similar to that for high solar activity condition. Similar variation in the emission intensities due to the change in EUV flux models for solar minimum and maximum conditions has been found on Mars [*Jain and Bhardwaj*, 2012].

[31] For all the three (low, moderate, and high) solar activity conditions, the contribution of PD of CO₂ to the Cameron band production is 50% higher when the S2K solar flux model is used. This is because of an order of magnitude higher solar EUV flux in the 1000–1050 Å bin in the S2K model compared to that in the EUVAC model. Solar EUV flux in the 1000–1050 Å bin does not significantly contribute to the photoionization, but mostly affects the PD of CO₂, thus affecting the Cameron band production in the PD of CO₂.

[32] For solar maximum condition, the calculated intensities using the EUVAC model are 2 times higher than those calculated for solar minimum condition. When the S2K model is used, the respective intensities of UV doublet and Cameron band emissions are 1.3 and 1.6 times larger in high solar activity than those in low solar activity condition. For the EUVAC solar flux model, the variation in contribution of electron impact processes is more prominent for change in solar activity from low to high due to a change of more than a factor of 2 in the solar EUV flux below 250 Å, whereas solar EUV flux in the S2K model varies by less than a factor of 2 from solar minimum to maximum condition.

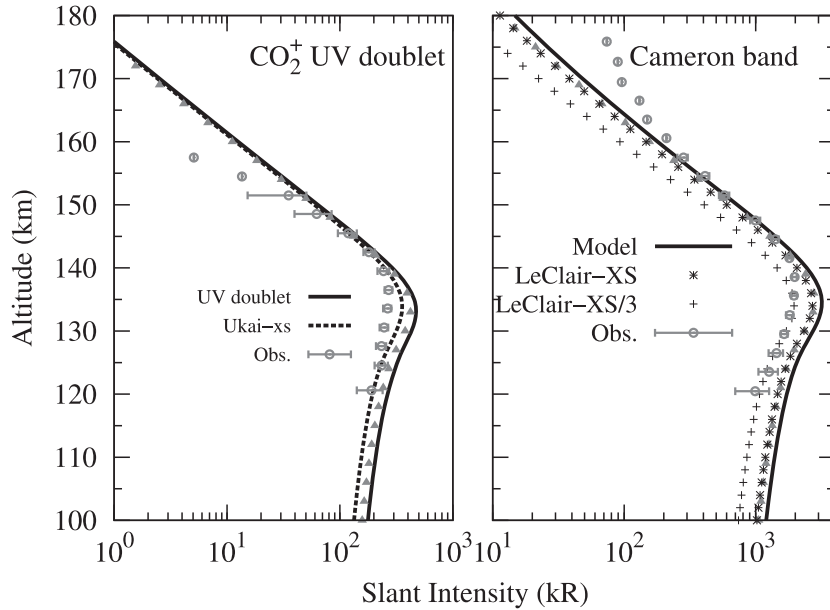


Figure 10. The calculated (using EUVAC solar flux model) limb profiles of CO_2^+ UV doublet and CO Cameron band emissions for conditions similar to SPICAV observations ($F_{10.7} = 144$ and $\text{SZA} = 25^\circ$) along with observed profiles taken from *Chaufray et al.* [2012]. Limb intensities of CO Cameron band, calculated by using the actual and corrected cross sections of $a^3\Pi$ state in e-CO process measured by *LeClair et al.* [1994], are also shown. Solid triangles show the calculated intensity on 8 October 2011 ($F_{10.7} = 118.3$ and $F_{10.7}$ 81 days average = 140.6, and $\text{SZA} = 25^\circ$). Limb intensity of CO_2^+ UV doublet calculated by using emission cross section of *Ukai et al.* [1992] is also shown (dashed curve).

4.2. $\text{CO}(a', d, e)$ Triplet Emissions on Venus

[33] The PD of CO_2 below 1080 Å leads to the formation of $\text{CO}(a^3\Pi)$, but at photon energies greater than 12.4 eV (wavelength < 1000 Å), other channels open up. The PD of CO_2 in the 10.3–13.8 eV (1200–900 Å) region leads to the channel $\text{CO}^* + \text{O}(^3\text{P})$, where CO^* corresponds to four triplet levels $a^3\Pi$, $a^3\Sigma^+$, $d^3\Delta$, and $e^3\Sigma^-$. Emissions arising due to the transition from the a' , d , and e states to the $a^3\Pi$ state are called Asundi, triplet, and Herman bands, respectively. *Conway* [1981] reported that the CO Cameron band spectra observed by Mariner showed a very hot rotational distribution. His analysis showed a bimodal fit with temperatures 1600 K and 10,000 K. Analysis of SPICAM/Mars Express data also showed similar hot distribution [*Kalogerakis et al.*, 2012].

[34] Recently, *Kalogerakis et al.* [2012] studied the PD of CO_2 in laboratory and found strong emissions in the visible and near-IR region arising from the $\text{CO}(a', d, e)$ triplet states. They attributed these triplet band emissions to be the primary source for the $\text{CO}(a-X)$ Cameron bands. *Kalogerakis et al.* [2012] concluded that most of the observed Cameron band arising from PD of CO_2 is preceded by the cascading from the $\text{CO}(a', d, e)$ triplet states and predicted that the visible and near-IR (6000 to >14000 Å) emissions from these triplet states are of the same magnitude as the CO Cameron band.

[35] Using the study of *Kalogerakis et al.* [2012], one can predict the lower limit of Asundi, triplet, and Herman bands in the atmosphere of Venus, if only PD of CO_2 is considered as the primary source of these $\text{CO}(a', d, e)$ triplet states. Results from the present study show that for solar minimum condition the contribution of PD of CO_2 to the CO Cameron

band production on Venus is 5.7 kR (see Table 2). Thus, the $\text{CO}(a', d, e)$ emissions would also be about 5.7 kR on Venus, spread over the 6000 to >14000 Å range. The Asundi $a' - a$ (5–0) band at 7830 Å is about 10% of the total triplet band emissions [*Kalogerakis et al.*, 2012], thus its overhead intensity on Venus would be about 570 R. Similarly, during the solar maximum condition, total intensity of $\text{CO}(a', d, e)$ triplet and Asundi $a' - a$ (5–0) bands on Venus would be 7.5 kR and 750 R, respectively. The maximum fraction of Cameron band originates from electron impact on CO_2 and CO on Venus and these processes do not exclude similar CO product [*Kalogerakis et al.*, 2012]. The magnitude of $\text{CO}(a', d, e)$ triplet bands on Venus reported above would be a lower limit; hence, an upper limit could be larger by a factor of 2 to 3.

4.3. Calculation of Other Ultraviolet Emissions

[36] Currently, after a prolonged minimum, the Sun is in the ascending phase of solar activity with moderate condition. As discussed in section 3.3, we have carried out model calculations for the moderate ($F_{10.7} = 130$) solar activity condition. For the SPICAV/VEx observation of UV dayglow emissions during the current solar moderate condition, our model predicts the CO Cameron band (CO_2^+ UV doublet) intensity of ~ 2200 kR (330 kR) at an altitude of ~ 135 km. Based on our earlier calculations of N_2 triplet band emissions on Venus [*Bhardwaj and Jain*, 2012a], in moderate solar activity condition, we predict the maximum intensity of about 10 kR for N_2 Vegard-Kaplan (0, 6) emission at the altitude of 135 km (see Figure 9). The N_2 VK (0, 6) emission at 2762 Å has been observed on Mars [*Leblanc et al.*, 2006] and is the brightest emission in the N_2 VK band system

[Jain and Bhardwaj, 2011; Bhardwaj and Jain, 2012a]. The intensity of other prominent transition of N_2 VK band can be calculated using the intensity ratio provided in our earlier calculations [Jain and Bhardwaj, 2011; Bhardwaj and Jain, 2012a, 2012b]. We have also calculated the limb intensity of N_2 VK band in the wavelength range 1500–3000 Å (that lies within the SPICAV UV measurement range), which is shown in Figure 9. The maximum limb intensity of N_2 VK band in the 1500–3000 Å range is about 60 kR for solar moderate activity condition.

[37] We have recently developed a model for visible atomic oxygen dayglow emissions in the atmosphere of Mars (Jain and Bhardwaj, manuscript in preparation, 2013). We have applied this model on Venus and calculated the atomic oxygen 2972 Å (which is within the SPICAV UV measurement range) emission on Venus for moderate solar activity condition. The calculated limb profile of O I 2972 Å emission is presented in Figure 9, which shows two peaks: the lower peak at ~ 115 km has intensity of 375 kR, while the upper peak at ~ 135 km has intensity of 154 kR. The upper peak is mainly due to the photodissociation of CO_2 at wavelengths between 860 and 1160 Å, while the lower peak is due to PD of CO_2 by solar H Ly- α photons (1216 Å). Recent analysis of SPICAM-observed O I 2972 Å emission profile on Mars also suggests a double peak structure [Gronoff *et al.*, 2012].

5. Comparison of Model Calculations With the Recent SPICAV Observation

[38] Within weeks of submitting this paper, *Chaufray et al.* [2012] reported the first dayglow observation of CO Cameron band and CO_2^+ UV doublet emissions on Venus by SPICAV aboard Venus Express. The SPICAV observations were made between October and December 2011, with solar zenith angles varying between 20° and 30° . We have carried out calculation for the similar condition as reported by *Chaufray et al.* [2012] by taking SZA of 25° and VTS3 model atmosphere for 15 November 2011 ($F_{10.7} = 148$ and $F_{10.7}$ 81 days average = 144). Figure 10 shows the calculated CO Cameron band and CO_2^+ UV doublet brightness profiles along with the SPICAV-observed profiles taken from *Chaufray et al.* [2012].

[39] The model-calculated brightness of CO Cameron band peaks at 134 km with a value of 3200 kR. The SPICAV-observed peak of Cameron band brightness is situated at 137 ± 1.5 km and the magnitude of limb intensity at this altitude is ~ 2000 kR [Chaufray *et al.*, 2012]. The calculated intensity at the peak is about 50% higher than the observed value. When the $CO(a^3\Pi)$ production cross section in e-CO collision of *LeClair et al.* [1994] is used, the limb intensity of Cameron band at the peak altitude is 2700 kR. As mentioned earlier, the cross section obtained by *LeClair et al.* [1994] might be overestimated by a factor of 3 (see section 2). On decreasing the *LeClair et al.* [1994] measured cross section by a factor of 3, the calculated CO Cameron band brightness at the peak is ~ 2000 kR. For CO_2^+ ultraviolet doublet emission, maximum limb intensity of ~ 470 kR is obtained at an altitude of 133 km, which is $\sim 70\%$ higher than the SPICAV-observed value of 270 kR (at 135.5 ± 2.5 km) [Chaufray *et al.*, 2012]. However, this difference is maximum at peak only. At altitudes above (below) the peak, say at 150 km

(120 km), the calculated intensity is in agreement with the SPICAM observation. If emission cross section of $CO_2(B^2\Sigma_u^+)$ given by *Ukai et al.* [1992] is used in the calculation, then calculated UV doublet emission intensity (see dashed curve in Figure 10) is $\sim 30\%$ higher than the observation. The observed profile of CO_2^+ UV doublet emission may contain a small portion of O I 2972 Å emission [Chaufray *et al.*, 2012], which makes the shape of observed brightness profile different than the calculated emission profile at lower altitudes. The comparison between calculation and observation depends on factors such as local variations in the neutral atmosphere density and temperature depending on $F_{10.7}$, winds, and vertical transport, averaging over 3 months to get the adequate S/N ratio for the observational profiles, and moreover uncertainty in the model calculation. For example, model-calculated intensities of CO Cameron band and CO_2^+ UV doublet emissions decrease by $\sim 13\%$ (see Figure 10) on 8 October 2011 ($F_{10.7} = 118.3$ and $F_{10.7}$ 81 days average = 140.6, and SZA = 25°).

[40] *Chaufray et al.* [2012] have derived the overhead intensity of 25.3 kR and 3.2 kR for Cameron band and CO_2^+ UV doublet emissions, respectively, by converting the limb intensity to zenith brightness above subsolar point. These values are significantly lower than our model calculated height-integrated overhead intensities of 70 and 8 kR (at SZA = 25°) for Cameron band and CO_2^+ UV doublet emissions, respectively. This discrepancy in the calculated and observation-derived overhead intensity is significant and it is difficult to reconcile or comment on the cause for this difference at present and further investigation is needed.

[41] The calculated altitude of peak brightness of both CO Cameron band and CO_2^+ UV doublet emissions is lower by ~ 5 km than the observation. The difference in peak altitude of observed and calculated emissions shows that the upper atmospheric neutral density is smaller in our model calculation. Recent general circulation model for Venus (VTGCM) also suggests that VTS3 empirical model is inadequate to properly represent lower thermosphere thermal structure [Brecht and Bougher, 2012]. Density profile of CO_2 calculated by VTGCM varies significantly from that calculated by VTS3 model above 100 km.

6. Summary and Conclusions

[42] We have presented the model calculation of CO Cameron band and CO_2^+ doublet ultraviolet emissions in the dayglow of Venus and assessed the impact of solar EUV flux model on the calculated intensities. The calculated volume production rates of CO Cameron band and CO_2^+ UV doublet emissions are height integrated to compute the overhead intensity and integrated along the line of sight to obtain the limb intensities for low, moderate, and high solar activity conditions. With updated cross section, the electron impact on CO is found to be the major source of $CO(a^3\Pi)$ production followed by electron and photon impact dissociation of CO_2 . The major source of CO_2^+ UV doublet emission in Venusian dayglow is photoionization of CO_2 followed by electron impact ionization of CO_2 . The contribution of fluorescence scattering by CO_2^+ to the CO_2^+ UV doublet emission is quite negligible. The calculated overhead intensities of CO Cameron band and CO_2^+ UV doublet emission are about a factor of 2 higher in the solar maximum condition than those

during the solar minimum condition. This variation in intensity from low to high solar activity depends upon the solar EUV flux model used in the calculation, e.g., when the S2K model is used instead of EUVAC, the emission intensities of CO Cameron band and CO₂⁺ UV doublet vary by less than a factor of 2. The effect of solar EUV flux models on the emission intensity is 30–40% in solar minimum condition and ~2–10% in solar maximum condition.

[43] For the SPICAV/VEx observation of UV dayglow emissions during the solar moderate condition, we have predicted the limb intensity of about 2400 and 300 kR for CO Cameron band and CO₂⁺ UV doublet emissions, respectively. We have also predicted the intensities of N₂ Vegard-Kaplan UV bands (~60 kR in wavelength range 1500–3000 Å, peaking at ~135 km) and O I 2972 Å emission (375 kR at lower (~115 km) and 155 kR at upper (~135 km) peak) in moderate solar activity condition.

[44] We have compared our calculated limb intensity of CO Cameron band and CO₂⁺ UV doublet emissions with the first observation of these emissions on Venus using SPICAV/VEx [Chaufray *et al.*, 2012]. The calculated intensity of CO Cameron band at the peak altitude is about 50% higher than the SPICAV observation. However, when the CO(a³Π) production cross section in e-CO collision measured by LeClair *et al.* [1994] is used in the model calculation, this difference reduces to 30% and with a correction by a factor of 3 in cross section, the magnitude of calculated brightness at peak is in good agreement with the observation. The calculated maximum brightness of CO₂⁺ doublet emission is ~70% higher than the SPICAV observation. However, when CO₂⁺(B) emission cross section of Ukai *et al.* [1992] is used, the calculated maximum intensity agrees better with the observation. We found that our calculated overhead intensities of the two emissions are significantly higher than those derived from the observations. It may be noted that a number of factors can affect the comparison between observation and calculation, e.g., observed brightness profiles are averaged of several measurements spanning over 3 months during which variation in the solar zenith angle and other local variations in neutral atmosphere and temperature can affect the dayglow emissions. Moreover, uncertainties in the model input parameters can also cause discrepancy between observed and calculated brightness profiles. Presently, it is difficult to comment on this discrepancy and further investigation is needed. Our model-calculated peak altitude of CO Cameron band and CO₂⁺ UV doublet emission profiles is lower than that observed by SPICAV, indicating lower neutral density in the VTS3 model atmosphere for Venus used in our calculation.

[45] The present study has clearly demonstrated that the cross section of a³Π state in e-CO process is important in modeling CO Cameron band emission on Mars and Venus. The contribution of e-CO process in CO Cameron band also depends on the density of CO in the atmosphere; hence, it is difficult to constrain the former without fixing the latter. Present calculation also showed that use of excitation and emission cross section of CO₂⁺(B) can affect the UV doublet emission intensity, and one should be careful while using these cross sections in the model calculation. A more detailed study of these emissions taking the Venus thermosphere general circulation model (VTGCM) needs to be carried out to understand the recent SPICAV observations.

[46] **Acknowledgments.** Sonal Kumar Jain was supported by Senior Research Fellowship of ISRO during the period of this work. We thank the reviewers for their useful suggestions and helpful comments that has improved the paper.

[47] Masaki Fujimoto thanks the reviewers for their assistance in evaluating this paper.

References

- Ajello, J. M. (1971a), Emission cross sections of CO₂ by electron impact in the interval 1260–4500 Å, *J. Chem. Phys.*, *55*, 3169–3177, doi:10.1063/1.1676564.
- Ajello, J. M. (1971b), Emission cross section of CO by electron impact in the interval 1260–5000 Å, *J. Chem. Phys.*, *55*, 3158–3168, doi:10.1063/1.1676563.
- Avakyan, S. V., R. N. Il'in, V. M. Lavrov, and G. N. Ogurtsov (1998), *Collision Processes and Excitation of UV Emission From Planetary Atmospheric Gases: A Handbook of Cross Sections*, edited by S. V. Avakyan, Gordon and Breach, India.
- Bertaux, J. L., J. E. Blamont, V. M. Lepine, V. G. Kurt, N. N. Romanova, and A. S. Smirnov (1981), Venera 11 and Venera 12 observations of EUV Emissions from the upper atmosphere of Venus, *Planet. Space Sci.*, *29*(2), 149–166.
- Bhardwaj, A. (1999), On the role of solar EUV, photoelectrons, and auroral electrons in the chemistry of C(¹D) and the production of CI 1931 Å in the inner cometary coma: A case for comet P/Halley, *J. Geophys. Res.*, *104*, 1929–1942, doi:10.1029/1998JE900004.
- Bhardwaj, A. (2003), On the solar EUV deposition in the inner comae of comets with large gas production rates, *Geophys. Res. Lett.*, *30*(24), 2244, doi:10.1029/2003GL018495.
- Bhardwaj, A., and S. K. Jain (2009), Monte Carlo model of electron energy degradation in a CO₂ atmosphere, *J. Geophys. Res.*, *114*, A11309, doi:10.1029/2009JA014298.
- Bhardwaj, A., and S. K. Jain (2012a), Calculations of N₂ triplet states vibrational populations and band emissions in Venusian dayglow, *Icarus*, *217*, 752–758, doi:10.1016/j.icarus.2011.05.026.
- Bhardwaj, A., and S. K. Jain (2012b), Production of N₂ Vegard-Kaplan and other triplet band emissions in the dayglow of Titan, *Icarus*, *218*(2), 989–1005, doi:10.1016/j.icarus.2012.01.019.
- Bhardwaj, A., and M. Michael (1999), Monte Carlo model for electron degradation in SO₂ gas: Cross sections, yield spectra and efficiencies, *J. Geophys. Res.*, *104*(10), 24,713–24,728, doi:10.1029/1999JA900283.
- Bhardwaj, A., and S. Raghuram (2011), Model for Cameron-band emission in comets: A case for the EPOXI mission target comet 103P/Hartley 2, *Mon. Not. R. Astron. Soc. Lett.*, *412*, L25–L29, doi:10.1111/j.1745-3933.2010.00998.x.
- Bhardwaj, A., S. A. Haider, and R. P. Singhal (1990), Auroral and photoelectron fluxes in cometary ionospheres, *Icarus*, *85*, 216–228, doi:10.1016/0019-1035(90)90112-M.
- Brecht, A. S., and S. W. Bougher (2012), Dayside thermal structure of Venus' upper atmosphere characterized by a global model, *J. Geophys. Res.*, *117*, E08002, doi:10.1029/2012JE004079.
- Broadfoot, A. L., S. Kumar, M. J. S. Belton, and M. B. McElroy (1974), Ultraviolet observations of Venus from Mariner 10: Preliminary results, *Science*, *183*, 1315–1318.
- Broadfoot, A. L., S. S. Clapp, and F. E. Stuart (1977), Mariner 10 ultraviolet spectrometer: Airglow experiment, *Space Sci. Instrum.*, *3*, 199–208.
- Chaufray, J.-Y., J.-L. Bertaux, and F. Leblanc (2012), First observation of the Venus UV dayglow at limb from SPICAV/VEX, *Geophys. Res. Lett.*, *39*, L20201, doi:10.1029/2012GL053626.
- Conway, R. R. (1981), Spectroscopy of the Cameron bands in the Mars airglow, *J. Geophys. Res.*, *86*, 4767–4775, doi:10.1029/JA086iA06p04767.
- Dalgarno, A., and T. C. Degges (1971), CO₂⁺ Dayglow on Mars and Venus, in *Planetary Atmospheres, Proceedings From 40th IAU Symposium Held in Marfa, Texas, 26–31 October 1969*, edited by Sagan, C., T. C. Owen, and H. J. Smith, vol. 40. pp. 337–345, Reidel, Springer-Verlag, New York.
- Erdman, P. W., and E. C. Zipf (1983), Electron-impact excitation of the Cameron system (a³Π → X¹Σ) of CO, *Planet. Space Sci.*, *31*, 317–321, doi:10.1016/0032-0633(83)90082-X.
- Fox, J. L. (2009), Morphology of the dayside ionosphere of Mars: Implications for ion outflows, *J. Geophys. Res.*, *114*, E12005, doi:10.1029/2009JE003432.
- Fox, J. L., and S. W. Bougher (1991), Structure, luminosity, and dynamics of the Venus thermosphere, *Space Sci. Rev.*, *55*, 357–489, doi:10.1007/BF00177141.
- Fox, J. L., and A. Dalgarno (1979), Ionization, luminosity, and heating of the upper atmosphere of Mars, *J. Geophys. Res.*, *84*, 7315–7333, doi:10.1029/JA084iA12p07315.

- Fox, J. L., and A. Dalgarno (1981), Ionization, luminosity and heating of upper atmosphere of Venus, *J. Geophys. Res.*, *86*, 629–639, doi:10.1029/JA086iA02p00629.
- Furlong, J. M., and W. R. Newell (1996), Total cross section measurement for the metastable $a^3\Pi$ state in CO, *J. Phys. B*, *29*, 331–338, doi:10.1088/0953-4075/29/2/020.
- Gérard, J.-C., B. Hubert, J. Gustin, V. I. Shematovich, D. Bisikalo, G. R. Gladstone, and L. W. Esposito (2011a), EUV spectroscopy of the Venus dayglow with UVIS on Cassini, *Icarus*, *211*(1), 70–80, doi:10.1016/j.icarus.2010.09.020.
- Gérard, J.-C., J. Gustin, B. Hubert, G. R. Gladstone, and L. W. Esposito (2011b), Measurements of the helium 584 Å airglow during the Cassini flyby of Venus, *Planet. Space Sci.*, *59*, 1524–1528, doi:10.1016/j.pss.2011.06.018.
- Gilijamse, J. J., S. Hoekstra, S. A. Meek, M. Metsälä, S. Y. T. van de Meerakker, G. Meijer, and G. C. Groenenboom (2007), The radiative lifetime of metastable CO ($a^3\Pi$, $v = 0$), *J. Chem. Phys.*, *127*, 221102, doi:10.1063/1.2813888.
- Gronoff, G., J. Liliensten, C. Simon, M. Barthélemy, F. Leblanc, and O. Dutuit (2008), Modelling the Venusian airglow, *Astron. Astrophys.*, *482*(3), 1015–1029, doi:10.1051/0004-6361:20077503.
- Gronoff, G., C. S. Wedlund, C. J. Mertens, M. Barthélemy, R. J. Lillis, and O. Witasse (2012), Computing uncertainties in ionosphere-airglow models. II—The Martian airglow, *J. Geophys. Res.*, *117*, A05309, doi:10.1029/2011JA017308.
- Hedin, A. E., H. B. Niemann, W. T. Kasprzak, and A. Seiff (1983), Global empirical model of the Venus thermosphere, *J. Geophys. Res.*, *88*(A1), 73–83, doi:10.1029/JA088iA01p00073.
- Hubert, B., J.-C. Gérard, J. Gustin, D. V. Bisikalo, V. I. Shematovich, and G. R. Gladstone (2012), Cassini-UVIS observation of dayglow FUV emissions of carbon in the thermosphere of Venus, *Icarus*, *220*, 635–646, doi:10.1016/j.icarus.2012.06.002.
- Jain, S. K., and A. Bhardwaj (2011), Model calculation of N₂ Vegard-Kaplan band emissions in Martian dayglow, *J. Geophys. Res.*, *116*, E07005, doi:10.1029/2010JE003778.
- Jain, S. K., and A. Bhardwaj (2012), Impact of solar EUV flux on CO Cameron band and CO₂ UV doublet emissions in the dayglow of Mars, *Planet. Space Sci.*, *63–64*, 110–122, doi:10.1016/j.pss.2011.08.010.
- Johnson, C. E. (1972), Lifetime of CO($a^3\Pi$) following electron impact dissociation of CO₂, *J. Chem. Phys.*, *57*(1), 576–577, doi:10.1063/1.1678007.
- Kalogerakis, K. S., C. Romanescu, M. Ahmed, K. R. Wilson, and T. G. Slanger (2012), CO prompt emission as a CO₂ marker in comets and planetary atmospheres, *Icarus*, *220*, 205–210, doi:10.1016/j.icarus.2012.04.028.
- Lawrence, G. (1972), Photodissociation of CO₂ to produce CO($a^3\Pi$), *J. Chem. Phys.*, *56*, 3435–3442, doi:10.1063/1.1677717.
- Leblanc, F., J. Y. Chaufray, J. Liliensten, O. Witasse, and J.-L. Bertaux (2006), Martian dayglow as seen by the SPICAM UV spectrograph on Mars Express, *J. Geophys. Res.*, *111*, E09S11, doi:10.1029/2005JE002664.
- LeClair, L. R., M. D. Brown, and J. W. McConkey (1994), Selective detection of O(¹S) and CO($a^3\Pi$) following electron impact on CO using solid xenon, *Chem. Phys.*, *189*, 769–777.
- LeCompte, M. A., L. J. Paxton, and A. I. F. Stewart (1989), Analysis and interpretation of observations of airglow at 297 nm in the Venus thermosphere, *J. Geophys. Res.*, *94*(A1), 208–216.
- Morgan, L. A., and J. Tennyson (1993), Electron impact excitation cross sections for CO, *J. Phys. B*, *26*, 2429–2441, doi:10.1088/0953-4075/26/15/026.
- Raghuram, S., and A. Bhardwaj (2012), Model for the production of CO Cameron band emission in Comet 1P/Halley, *Planet. Space Sci.*, *63–64*, 139–149, doi:10.1016/j.pss.2011.11.011.
- Richards, P. G., J. A. Fennelly, and D. G. Torr (1994), EUVAC: A solar EUV flux model for aeronomic calculations, *J. Geophys. Res.*, *99*, 8981–8992, doi:10.1029/94JA00518.
- Schunk, R. W., and A. F. Nagy (2000), *Ionospheres: Physics, Plasma Physics, and Chemistry*, Cambridge Univ. Press, Cambridge, U.K.
- Seiersen, K., A. Al-Khalili, O. Heber, M. J. Jensen, I. B. Nielsen, H. B. Pedersen, C. P. Safvan, and L. H. Andersen (2003), Dissociative recombination of the cation and dication of CO₂, *Phys. Rev. A*, *68*(2), 022708, doi:10.1103/PhysRevA.68.022708.
- Simon, C., O. Witasse, F. Leblanc, G. Gronoff, and J.-L. Bertaux (2009), Dayglow on Mars: Kinetic modeling with SPICAM UV limb data, *Planet. Space Sci.*, *57*, 1008–1021, doi:10.1016/j.pss.2008.08.012.
- Singhal, R. P., and A. Bhardwaj (1991), Monte Carlo simulation of photoelectron energization in parallel electric fields: Electrogrow on Uranus, *J. Geophys. Res.*, *96*, 15,963–15,972, doi:10.1029/90JA02749.
- Singhal, R. P., C. Jackman, and A. E. S. Green (1980), Spatial aspects of low and medium energy electron degradation in N₂, *J. Geophys. Res.*, *85*(A3), 1246–1254, doi:10.1029/JA085iA03p01246.
- Skrzypkowski, M. P., T. Gougousi, R. Johnsen, and M. F. Golde (1998), Measurement of the absolute yield of CO($a^3\Pi$)+O products in the dissociative recombination of CO₂⁺ ions with electrons, *J. Chem. Phys.*, *108*, 8400–8407, doi:10.1063/1.476267.
- Tobiska, W. K. (2004), SOLAR2000 irradiances for climate change, aeronomy and space system engineering, *Adv. Space Res.*, *34*, 1736–1746, doi:10.1016/j.asr.2003.06.032.
- Ukai, M., K. Kameta, N. Kouchi, K. Nagano, and Y. Hatano (1992), Autoionizing-resonance enhanced preferential photodissociation of CO₂ in superexcited states, *J. Chem. Phys.*, *97*(5), 2835–2842, doi:10.1063/1.463026.
- Wells, W. C., W. L. Borst, and E. C. Zipf (1972), Production of CO($a^3\Pi$) and other metastable fragments by electron impact dissociation of CO₂, *J. Geophys. Res.*, *77*(1), 69–75, doi:10.1029/JA077i001p00069.